ORIGINAL ARTICLE
DOI: 10.5433/1679-0375.2022v43n1Espp51

Numerical convergence of a Telegraph Predator-Prey system

Convergência numérica de um sistema de equações Telegráficas Predador-Presa

Kariston Stevan Luiz[1]; Juniormar Organista[2]; Eliandro Rodrigues Cirilo[3]; Neyva Maria Lopes Romeiro[4]; Paulo Laerte Natti[5]

Abstract

Numerical convergence of a Telegraph Predator-Prey system is studied. This partial differential equation (PDE) system can describe various biological systems with reactive, diffusive, and delay effects. Initially, the PDE system was discretized by the Finite Differences method. Then, a system of equations in a time-explicit form and in a space-implicit form was obtained. The consistency of the Telegraph Predator-Prey system discretization was verified. Von Neumann stability conditions were calculated for a Predator-Prey system with reactive terms and for a Delayed Telegraph system. On the other hand, for our Telegraph Predator-Prey system, it was not possible to obtain the von Neumann conditions analytically. In this context, numerical experiments were carried out and it was verified that the mesh refinement and the model parameters, reactive constants, diffusion coefficients and delay constants, determine the stability/instability conditions of the discretized equations. The results of numerical experiments were presented.

Keywords: Reactive-Diffusive-Telegraph system, Maxwell-Cattaneo delay, discretization consistency, Von Neumann stability, numerical experimentation.

Resumo

Estuda-se a convergência numérica de um sistema Predador-Presa Telegráfico. Esse sistema de equações diferenciais parciais (EDP) pode descrever vários sistemas biológicos com efeitos reativos, difusivo e de retardo. Inicialmente o sistema de EDPs foi discretizado pelo método de Diferenças Finitas. Então, um sistema de equações em uma forma explícita no tempo e em uma forma ímplicita no espaço foi obtido. A consistência da discretização do sistema Predador-Presa Telegráfico foi verificada. A seguir, as condições de estabilidade de von Neumann foram calculadas para um sistema predador-presa com termos reativos e para um sistema telegráfico com retardo. Por outro lado, para o nosso sistema Predador-Presa Telegráfico não foi possível obter analiticamente as condições de von Neumann. Neste contexto foram realizados experimentos numéricos e verificou-se que o refinamento da malha e os parâmetros do modelo, as constantes reativas, coeficientes de difusão e constantes de retardo, determinam as condições de estabilidade/instabilidade das equações discretizadas. Os resultados das experimentações numéricas foram apresentados.

Palavras-chave: Sistema Telegráfico-Difusivo-Reativo, retardo de Maxwell-Cattaneo, consistência da discretização, estabilidade de Von Neumann, experimentação numérica.

[1] Ms. Kariston Stevan Luiz, Mathematics Depto., UEL, Londrina, PR., Brazil, E-mail: kslpgmac@gmail.com
[2] Ms. Juniormar Organista, Mathematics Depto., UEL, Londrina, PR., Brazil, E-mail: juniormarorganista@gmail.com
[3] Prof. Dr. Eliandro Rodrigues Cirilo, Mathematics Depto., UEL, Londrina, PR., Brazil, E-mail: ercirilo@uel.br
[4] Prof. Dr. Neyva Maria Lopes Romeiro, Mathematics Depto., UEL, Londrina, PR., Brazil, E-mail: nromeiro@uel.br
[5] Prof. Dr. Paulo Laerte Natti, Mathematics Depto., UEL, Londrina, PR., Brazil, E-mail: plnatti@uel.br

Introduction

Currently, there is a growing interest in the study of population dynamics, mainly due to the need to have better control of epidemics (ABIDEMI; ZAINIDDIN; AZIZ, 2021; CIRILO *et al.*, 2021a; CIRILO *et al.*, 2021b; PAUL *et al.*, 2021), or to reduce the economic, biological and social losses caused by invasive species (ASH *et al.*, 2022; KISHORE *et al.*, 2021; LI; YUAN; WANG, 2023), among other needs.

The first mathematical studies aimed at describing interactions between populations took place in the 1920s (BAZYKIN, 1998). During this period, the Lotka-Volterra mathematical model emerged (LOTKA, 1925; VOLTERRA, 1926). This model describes the predator-prey interaction between two populations through the system of ordinary differential equations, given by

$$\begin{aligned} \frac{dS_1}{dt} &= a_1 S_1 - c_1 S_1 S_2 \\ \frac{dS_2}{dt} &= -a_2 S_2 + c_2 S_1 S_2, \end{aligned} \tag{1}$$

where $S_1 > 0$ and $S_2 > 0$ denote the population densities of the interacting species, with S_1 being the density of prey and S_2 the density of predators. Furthermore, $a_1 > 0$ is the birth rate of the species S_1, $a_2 > 0$ is the death rate of the species S_2, and the parameters $c_1 > 0$ and $c_2 > 0$ are the interaction rates between the two species. The non-derivative terms on the right side of the system, equation (1), are called reactive terms.

Later in the 1950s, Holling carried out experiments to investigate how the rate of prey capture by a predator is related to the density of the prey (HOLLING, 1959a; HOLLING, 1959b), a relationship called the functional response.

Holling identified three general categories of functional responses, Figure 1. The type 1 functional response is linear, when the number of prey consumed increases in direct proportion to prey density. The type 2 functional response says that as the prey population increases, predators become satiated and consume a constant number of prey (saturation). The type 3 functional response is similar to type 2, except at low prey density, when prey switching effects occur (TANSKY, 1978).

Still in the 1950s, Huffaker investigated the effects of spatial structure on the interaction of mite populations.

Figure 1 – The three types of functional responses identified by Holling.

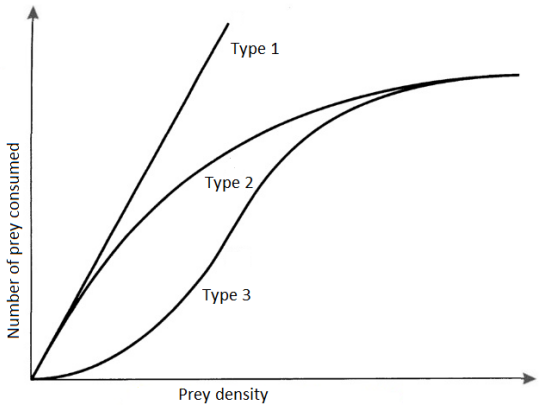

Source: Adapted by Holling (1959a).

Among several results, Huffaker showed that the predator-prey interaction could not survive in a homogeneous environment without dispersion (HUFFAKER, 1958).

Currently, through more complex mathematical modeling, there are works that emphasize the studies of the dynamics of invasive species, epidemics and other biological phenomena (BEARUP; PETROVSKAYA; PETROVSKII, 2015; CIRILO *et al.*, 2019; DE ROOS; MCCAULEY; WILSON, 1991; GREENHALGH; KHAN; PETTI, 2017; LEWIS; PETROVSKII; POTTS, 2016; LI; Li; YANG, 2016; TILLES; PETROVSKII; NATTI, 2016; TILLES; PETROVSKII; NATTI, 2017).

As the description of the effects of predating on one species by another improved, the mathematical models became more complex. Thus, in parallel with the development of more realistic and complex biological models, studies on the convergence of numerical methods applied to these models have become essential.

The Lax Equivalence Theorem is fundamental for the analysis of the convergence of numerical solutions of PDEs. The theorem says that in a well-posed initial value problem that has been consistently discretized, stability of the numerical method is a necessary and sufficient condition for numerical convergence (LAX; RICHTMYER, 1956).

About stability of numerical methods, it is associated with the propagation of numerical errors in the iterative process (HIRSCH, 2007). The numerical method is said to be stable if the errors decrease along the iterative process, otherwise, if the errors increase, the numerical solution will diverge and the numerical method is said to be unstable. Finally, a numerical method is said to be conditionally stable if it depends on certain parameters so that the errors remain limited.

In the case of linear problems, the von Neumann stability analysis is widely used (CUMINATO; MENEGUETTE, 1999). In the case of nonlinear initial condition problems, the stability of a numerical method can hardly be verified analytically (ISAACSON; KELLER, 1994). In such situations, numerical experiments are used to analyze the stability of the numerical method used (OLIVEIRA *et al.*, 2019).

About consistency of numerical method, we say that a discretized problem is consistent when it tends to the original differential equation if the increments in the independent variables tend to zero (SANGAY, 2015).

In this context, the objective of this work is to verify the consistency and stability of a numerical method applied to a Telegraph Predator-Prey system. The conditions for the convergence of the numerical model are analyzed through numerical experiments.

Modeling the Telegraph Predator-Prey system

In this section, the Maxwell-Cattaneo Diffusion equation system is first modeled and then the Telegraph Predator-Prey equation system is developed.

Maxwell-Cattaneo Diffusion system

The classical law of diffusion, Fick's law (PAUL *et al.*, 2014), is a law that describes the diffusion of a property in systems that are not in equilibrium. In systems where there are concentration gradients of a property, then there is a flow of this property which tends to homogenize the system.This homogenizing flow will go in the opposite direction of the gradient and, if this flow is weak, it can be approximated by the first term of a Taylor series, resulting in Fick's law. In the case of a Predator-Prey system in one dimension, this modeling is expressed mathematically by (PAUL *et al.*, 2014),

$$J_j = -D_j \frac{\partial S_j}{\partial x}, \tag{2}$$

where flow J_1 is due to diffusion of population density of prey S_1 and flow J_2 is due to diffusion of population density of predator S_2, while D_1 and D_2 are the diffusivity coefficients for prey and predators, respectively. Note that the negative sign, in equation (2), indicates that the homogenizing flow occurs in the opposite direction of the concentration gradient, ie, from high concentrations to low concentrations.

On the other hand, Fick's law proposes that signals propagate with infinite speed, which in practice does not happen, configuring the so-called "Paradox of Fourier's law" (MICKENS; JORDAN, 2003). To correct this problem, Fick's law is modified by the Maxwell-Cattaneo Diffusion law (CATTANEO, 1958) which introduces a lag time τ for each action. Thus, due to the finite speed of propagation of information, the system does not react instantly to an action.

For predator-prey systems, the Maxwell-Cattaneo Diffusion law is given by (CIRILO *et al.*, 2019)

$$\left(1+\tau_j \frac{\partial}{\partial t}\right) J_j = -D_j \frac{\partial S_j}{\partial x}, \tag{3}$$

where τ_1 is the reaction time of the prey when exposed to predating and τ_2 is the predator's reaction time to capture prey. Note that, contrary to the system (1), in the system (3) we have $S_j = S_j(x,t)$, for $j = 1,2$, so that now the population densities of prey and predator, respectively, also depend on the spatial variable x.

Telegraph Predator-Prey system

For predator-prey systems, in the context of Huffaker's hypotheses, the Maxwell-Cattaneo diffusion law must be incorporated into the population density conservation law. According to the Conservation Principle, the rate of change of a property in a volume V must be equal to the net flux of that property through the surface of V, plus the amount of the property transformed into the interior of V due to reactive effects (FORTUNA, 2012). Thus, the conservation equation for predator-prey system, considering diffusive, reactive and delay effects, is written as

$$\frac{\partial S_j}{\partial t} = -\frac{\partial J_j}{\partial x} + F_j\left(S_j\right), \tag{4}$$

where J_j are the population flows described by system (3) and $F_j(t,x,S)$ represents the prey reaction term, if $j = 1$, and the predator reaction term, if $j = 2$. Note that the equation (4) is a transport equation.

Therefore, deriving equation (4) with respect to time t and equation (3) with respect to coordinate x, we have

$$\frac{\partial^2 S_j}{\partial t^2} = -\frac{\partial}{\partial t}\left(\frac{\partial J_j}{\partial x}\right) + \frac{\partial}{\partial t} F_j\left(S_j\right) \tag{5}$$

$$\tau_j \frac{\partial}{\partial x}\left(\frac{\partial J_j}{\partial t}\right) + \frac{\partial J_j}{\partial x} = -D_j \frac{\partial^2 S_j}{\partial x^2}. \tag{6}$$

Noting that $F_j = F_j(S_j,x,t)$ and $S_j = S_j(x,t)$, it follows from the chain rule that

$$\frac{\partial}{\partial t}F_j(S_j) = \frac{d}{dS_j}F_j(S_j)\ \frac{\partial S_j}{\partial t}, \tag{7}$$

so that equation (5) is rewritten as

$$\frac{\partial^2 S_j}{\partial t^2} = -\frac{\partial}{\partial t}\left(\frac{\partial J_j}{\partial x}\right) + \frac{d}{dS_j}F_j(S_j)\ \frac{\partial S_j}{\partial t}. \tag{8}$$

Multiplying equation (8) by τ_j, and subtracting the resulting equation from equation (6), it follows that

$$\tau_j\frac{\partial^2 S_j}{\partial t^2} - \tau_j\frac{d}{dS_j}F_j(S_j)\ \frac{\partial S_j}{\partial t} = D_j\frac{\partial^2 S_j}{\partial x^2} + \frac{\partial J_j}{\partial x}. \tag{9}$$

Finally, obtaining $\frac{\partial J_j}{\partial x}$ from equation (4) and substituting in equation (9), we obtain the delayed predator-prey equations, whose population densities S_j are subject to reactive-diffusive processes (CIRILO *et al.*, 2019; MENDEZ; FEDOTOV; HORSTHEMKE, 2010), i.e.,

$$\tau_j\frac{\partial^2 S_j}{\partial t^2} + \left[1 - \tau_j\frac{d}{dS_j}F_j(S_j)\right]\frac{\partial S_j}{\partial t} = D_j\frac{\partial^2 S_j}{\partial x^2} + F_j(S_j). \tag{10}$$

The equations (10) will be designated in the remaining of the work as Telegraph Predator-Prey equations. Note that the equations (10) have the same structure as the classical Telegraph equation, which describe the propagation of electrical signals in long conducting cables.

Discretization of the Telegraph Predator-Prey system

Consider the equations (10) with the following initial and boundary conditions

$$\tau_1\frac{\partial^2 S_1}{\partial t^2} + \left[1 - \tau_1\frac{dF_1}{dS_1}\right]\frac{\partial S_1}{\partial t} = D_1\frac{\partial^2 S_1}{\partial x^2} + F_1 \tag{11}$$

$$\tau_2\frac{\partial^2 S_2}{\partial t^2} + \left[1 - \tau_2\frac{dF_2}{dS_2}\right]\frac{\partial S_2}{\partial t} = D_2\frac{\partial^2 S_2}{\partial x^2} + F_2 \tag{12}$$

$$S_j(x,0) = S_j^0\ ,\ \left.\frac{\partial S_j(x,t)}{\partial t}\right|^{t=0} = 0\ ,\ \forall x \in [0,L] \tag{13}$$

$$S_j(0,t) = S_j(L,t) = 0\ ,\ \forall t \in [0,T]\ ,\ j = 1,2, \tag{14}$$

where t and x are the temporal and spatial variables, τ_1 and τ_2 are the delay parameters of the populations, D_1 and D_2 are the diffusivity coefficients of the populations, $S_1(x,t)$ and $S_2(x,t)$ are the population densities, finally F_1 and F_2 are the prey and predator reactive terms of the populations, respectively. In this work, it is considered that the reactive terms present functional responses of the Holling 1 type, see Figure 1, i.e.,

$$F_1 = F_1(S_1,S_2) = a_1S_1 - b_1S_1^2 - c_1S_1S_2 \tag{15}$$

$$F_2 = F_2(S_1,S_2) = -a_2S_2 + c_2S_1S_2, \tag{16}$$

where a_1 is the prey birth rate, b_1 is the prey saturation term, c_1 is the prey death rate due to predating, a_2 is the predator death rate in the absence of prey and c_2 is the predator birth rate due to predating (NATTI *et al.*, 2019).

The initial conditions S_1^0 and S_2^0 are the initial population densities of prey and predators, respectively. Finally, the Dirichlet boundary conditions, equation (14), impose that at the boundary of the problem domain, the population densities are null.

To discretize the Telegraph Predator-Prey equations (11) and (12) the one-dimensional mesh shown in Figure 2 is used.

Cardinal point notation is used in the discretization of the problem domain. The labels P, W and E stand for center (P point where the calculation is performed), east and west, respectively. Lowercase acronyms are cardinal variations from the center P. As shown in Figure 2, the population densities S_1 and S_2 are calculated at the center of the cell. Note that storage shifted to population densities has a positive impact on numerical computation, reducing numerical instability (CIRILO *et al.*, 2018; FERREIRA *et al.*, 2001; FORTUNA, 2012; GRIEBEL; DORNSEIFER; NEUNHOEFFER, 1998; SAITA *et al.*, 2021).

As for the numerical method for discretizing the PDEs, the Finite Difference Technique was used (BURDEN; FAIRES, 2008; CUMINATO; MENEGUETTE, 1999). Thus, central finite differences are used for the discretization of the second derivatives, that is,

$$\left.\left(\frac{\partial^2 S_j}{\partial t^2}\right)\right|_P^k \approx \frac{1}{(\Delta t)^2}\left(S_j|_P^{k+1} - 2S_j|_P^k + S_j|_P^{k-1}\right) \tag{17}$$

$$\left.\left(\frac{\partial^2 S_j}{\partial x^2}\right)\right|_P^k \approx \frac{1}{(\Delta x)^2}\left(S_j|_E^k - 2\,S_j|_P^k + S_j|_W^k\right), \tag{18}$$

while for the first derivative in time, regressive finite differences are used

$$\left.\left(\frac{\partial}{\partial t}S_j\right)\right|_P^k \approx \frac{1}{\Delta t}\left(S_j|_P^k - S_j|_P^{k-1}\right). \tag{19}$$

Figure 2 – Discrete one-dimensional mesh used for the Telegraph Predator-Prey system.

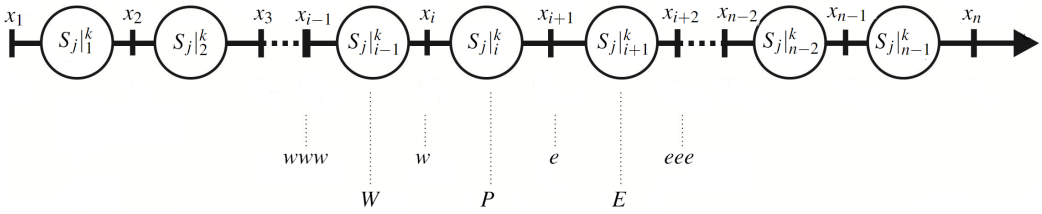

Source: The authors.

Finally, for the equation (11), it is still necessary to discretize the term

$$\left(\left[1-\tau_1\frac{\partial}{\partial S_1}F_1\left(S_1,S_2\right)\right]\frac{\partial S_1}{\partial t}\right)\Bigg|_P^k=$$

$$\left(\frac{\partial S_1}{\partial t}\right)\Bigg|_P^k-\tau_1\left(\frac{\partial}{\partial S_1}F_1\left(S_1,S_2\right)\right)\Bigg|_P^k\left(\frac{\partial S_1}{\partial t}\right)\Bigg|_P^k. \quad (20)$$

From equation (15), it follows that

$$\left(\frac{\partial}{\partial S_1}F_1\left(S_1,S_2\right)\right)\Bigg|_P^k=a_1-2b_1\,S_1|_P^k-c_1\,S_2|_P^k, \quad (21)$$

then using the equations (19) and (21) in the equation (20), one obtains that

$$\left(\frac{\partial}{\partial S_1}F_1\left(S_1,S_2\right)\frac{\partial S_1}{\partial t}\right)\Bigg|_P^k\approx$$

$$\left(a_1-2b_1\,S_1|_P^k-c_1\,S_2|_P^k\right)\left(\frac{1}{\Delta t}\left(S_1|_P^k-S_1|_P^{k-1}\right)\right)\approx$$

$$\frac{1}{\Delta t}\left(a_1\,S_1|_P^k-2b_1\,S_1^2|_P^k-c_1\,S_1|_P^k\,S_2|_P^k\right.$$

$$\left.-\,a_1\,S_1|_P^{k-1}+2b_1\,S_1|_P^{k-1}\,S_1|_P^k+c_1\,S_1|_P^{k-1}\,S_2|_P^k\right). \quad (22)$$

Substituting the equations (15), (17)-(19) and (22) in equation (11), it follows that the discretization of the prey equation is given by

$$S_1|_P^{k+1}=\Omega_1\left(\Upsilon_1 S_1|_W^k+\Pi_1 S_1^2|_P^k+\Phi_1 S_1|_P^k+\Lambda_1 S_1|_E^k+\Gamma_1\right) \quad (23)$$

where

$$\Upsilon_1=-\frac{D_1}{\Delta x^2}\quad,\quad\Lambda_1=-\frac{D_1}{\Delta x^2} \quad (24)$$

$$\Omega_1=-\frac{\Delta t^2}{\tau_1}\quad,\quad\Pi_1=\frac{2\tau_1 b_1}{\Delta t}+b_1 \quad (25)$$

$$\Phi_1=\frac{1-\tau_1\left(a_1-c_1S_2|_P^k+2b_1S_1|_P^{k-1}\right)}{\Delta t}+\frac{2\tau_1}{\Delta t^2}+\frac{2D_1}{\Delta x^2}$$

$$-a_1+c_1S_2|_P^k \quad (26)$$

$$\Gamma_1=\frac{\tau_1 S_1|_P^{k-1}}{\Delta t^2}-\frac{\left(1-\tau_1\left(a_1-c_1S_2|_P^k\right)\right)S_1|_P^{k-1}}{\Delta t}. \quad (27)$$

Note that the discretized prey equation (23) is explicit in time and implicit in space.

In a similar way, the formula for the discretization of the predator equation is obtained. The only difference is in the derivation of the predator reactive term, from equation (16),

$$\left(\frac{\partial}{\partial S_2}F_2\left(S_1,S_2\right)\right)\Bigg|_P^k=-a_2+c_2\,S_1|_P^k. \quad (28)$$

So the equation for discretizing the predator equation is given by

$$S_2|_P^{k+1}=\Omega_2\left(\Upsilon_2 S_2|_W^k+\Phi_2 S_2|_P^k+\Lambda_2 S_2|_E^k+\Gamma_2\right), \quad (29)$$

where

$$\Upsilon_2=-\frac{D_2}{\Delta x^2}\quad,\quad\Lambda_2=-\frac{D_2}{\Delta x^2}\quad,\quad\Omega_2=-\frac{\Delta t^2}{\tau_2} \quad (30)$$

$$\Phi_2=\frac{1-\tau_2(-a_2+c_2S_1|_P^k)}{\Delta t}-\frac{2\tau_2}{\Delta t^2}+\frac{2D_2}{\Delta x^2}+a_2-c_2S_1|_P^k \quad (31)$$

$$\Gamma_2=\frac{\tau_2 S_2|_P^{k-1}}{\Delta t^2}-\frac{\left(1-\tau_2(-a_2+c_2S_1|_P^k)\right)S_2|_P^{k-1}}{\Delta t}. \quad (32)$$

Again, note that the discretized prey equation (29) is explicit in time and implicit in space.

Numerical model consistency

The numerical solution of a problem does not always tend to the exact solution of the same problem. The resulting error between the exact solution of the continuous problem and the numerical solution obtained from the discretized equations is called local truncation error (LTE) (CUMINATO; MENEGUETTE, 1999). In most of the applied problems, the exact solution is not known and this is our case. In such situations one can estimate the Local Truncation Error through Taylor Series (BURDEN; FAIRES, 2008) and use this estimate to prove that the method is consistent at the limit of the continuum, when $\Delta x, \Delta t \to 0$.

Consider PDEs equations (11) and (12) and using the Finite Difference method, we have the following discretized equations

$$\frac{\tau_1}{\Delta t^2}\left(S_1\Big|_P^{k+1}-2S_1\Big|_P^{k}+S_1\Big|_P^{k-1}\right)$$
$$+\frac{1}{\Delta t}\left[\left(1-\tau_1\left(a_1-c_1\,S_2|_P^k-2b_1\,S_1|_P^k\right)\right)S_1|_P^k\right.$$
$$\left.-\left(1-\tau_1\left(a_1-c_1\,S_2|_P^k-2b_1\,S_1|_P^k\right)\right)S_1|_P^{k-1}\right]$$
$$-\frac{D_1}{\Delta x^2}\left(S_1\Big|_E^{k}-2S_1\Big|_P^{k}+S_1\Big|_W^{k}\right)-F_1\Big|_P^k=0 \quad (33)$$

and

$$\frac{\tau_2}{\Delta t^2}\left(S_2\Big|_P^{k+1}-2S_2\Big|_P^{k}+S_2\Big|_P^{k-1}\right)$$
$$+\frac{1}{\Delta t}\left[\left(1-\tau_2\left(-a_2+c_2\,S_1|_P^k\right)\right)S_2|_P^k\right.$$
$$\left.-\left(1-\tau_2\left(-a_2+c_2\,S_1|_P^k\right)\right)S_2|_P^{k-1}\right]$$
$$-\frac{D_2}{\Delta x^2}\left(S_2\Big|_E^{k}-2S_2\Big|_P^{k}+S_2\Big|_W^{k}\right)-F_2\Big|_P^k=0, \quad (34)$$

where F_1 and F_2 are the prey and predator reactive terms, equations (15) and (16), respectively.

Assuming that $W=P-\Delta x$ and $E=P+\Delta x$, let the Taylor Series expansions of the population densities in equations (33) and (34) be calculated around k and P, that is,

$$S_j\Big|_P^{k+1}=S_j\Big|_P^{k}+\Delta t\frac{\partial S_j}{\partial t}\Big|_P^k+\frac{(\Delta t)^2}{2}\frac{\partial^2 S_j}{\partial t^2}\Big|_P^k+\frac{(\Delta t)^3}{3!}\frac{\partial^3 S_j}{\partial t^3}\Big|_P^k$$
$$+\mathscr{O}(\Delta t^4), \quad (35)$$

$$S_j\Big|_P^{k-1}=S_j\Big|_P^{k}-\Delta t\frac{\partial S_j}{\partial t}\Big|_P^k+\frac{(\Delta t)^2}{2}\frac{\partial^2 S_j}{\partial t^2}\Big|_P^k-\frac{(\Delta t)^3}{3!}\frac{\partial^3 S_j}{\partial t^3}\Big|_P^k$$
$$+\mathscr{O}(\Delta t^4), \quad (36)$$

$$S_j\Big|_W^{k}=S_j\Big|_P^{k}-\Delta x\frac{\partial S_j}{\partial x}\Big|_P^k+\frac{(\Delta x)^2}{2}\frac{\partial^2 S_j}{\partial x^2}\Big|_P^k-\frac{(\Delta x)^3}{3!}\frac{\partial^3 S_j}{\partial x^3}\Big|_P^k$$
$$+\mathscr{O}(\Delta t^4), \quad (37)$$

$$S_j\Big|_E^{k}=S_j\Big|_P^{k}+\Delta x\frac{\partial S_j}{\partial x}\Big|_P^k+\frac{(\Delta x)^2}{2}\frac{\partial^2 S_j}{\partial x^2}\Big|_P^k+\frac{(\Delta x)^3}{3!}\frac{\partial^3 S_j}{\partial x^3}\Big|_P^k$$
$$+\mathscr{O}(\Delta t^4). \quad (38)$$

Substituting the equations (35)-(38) in the equations (33) and (34), with their respective $j=1,2$, we obtain that

$$\underbrace{\tau_1\frac{\partial^2 S_1}{\partial t^2}\Big|_P^k+\left[1-\tau_1\frac{dF_1}{dS_1}\Big|_P^k\right]\frac{\partial S_1}{\partial t}\Big|_P^k-D_1\frac{\partial^2 S_1}{\partial x^2}\Big|_P^k-F_1\Big|_P^k}_{\text{PDE}}$$
$$=\underbrace{\frac{\Delta t}{2}\left(1-\tau_1\frac{dF_1}{dS_1}\Big|_P^k\right)\frac{\partial^2 S_1}{\partial t^2}\Big|_P^k-\frac{\Delta t^2}{3!}\left(1-\tau_1\frac{dF_1}{dS_1}\Big|_P^k\right)\frac{\partial^3 S_1}{\partial t^3}\Big|_P^k}_{\text{local truncation error}}$$
$$+\underbrace{\left(1-\tau_1\frac{dF_1}{dS_1}\Big|_P^k\right)\mathscr{O}(\Delta t^3)-2\tau_1\mathscr{O}(\Delta t^2)+2D_1\mathscr{O}(\Delta x^2)}_{\text{local truncation error}} \quad (39)$$

and

$$\underbrace{\tau_2\frac{\partial^2 S_2}{\partial t^2}\Big|_P^k+\left[1-\tau_2\frac{dF_2}{dS_2}\Big|_P^k\right]\frac{\partial S_2}{\partial t}\Big|_P^k-D_2\frac{\partial^2 S_2}{\partial x^2}\Big|_P^k-F_2\Big|_P^k}_{\text{PDE}}$$
$$=\underbrace{\frac{\Delta t}{2}\left(1-\tau_2\frac{dF_2}{dS_2}\Big|_P^k\right)\frac{\partial^2 S_2}{\partial t^2}\Big|_P^k-\frac{\Delta t^2}{3!}\left(1-\tau_2\frac{dF_2}{dS_2}\Big|_P^k\right)\frac{\partial^3 S_2}{\partial t^3}\Big|_P^k}_{\text{local truncation error}}$$
$$+\underbrace{\left(1-\tau_2\frac{dF_2}{dS_2}\Big|_P^k\right)\mathscr{O}(\Delta t^3)-2\tau_2\mathscr{O}(\Delta t^2)+2D_2\mathscr{O}(\Delta x^2)}_{\text{local truncation error}}. \quad (40)$$

Finally, taking the limit of the continuum, when $\Delta t,\Delta x\to 0$, the equations (39) and (40) tend to

$$\tau_1\frac{\partial^2 S_1}{\partial t^2}\Big|_P^k+\left[1-\tau_1\frac{dF_1}{dS_1}\Big|_P^k\right]\frac{\partial S_1}{\partial t}\Big|_P^k-D_1\frac{\partial^2 S_1}{\partial x^2}\Big|_P^k-F_1\Big|_P^k=0 \quad (41)$$

and

$$\tau_2\frac{\partial^2 S_2}{\partial t^2}\Big|_P^k+\left[1-\tau_2\frac{dF_2}{dS_2}\Big|_P^k\right]\frac{\partial S_2}{\partial t}\Big|_P^k-D_2\frac{\partial^2 S_2}{\partial x^2}\Big|_P^k-F_2\Big|_P^k=0. \quad (42)$$

Note that the equations (41) and (42) are the PDEs (11) and (12), calculated at the mesh point P and at the instant k. It is concluded that the discretized equations (23) and (29), or equivalently equations (33) and (34), are consistent with the PDEs (11) and (12), respectively.

Numerical model stability

The von Neumann stability condition is based on the superposition principle, that is, which the error is the superposition of the errors accumulated at each iteration (CRANK; NICOLSON, 1947).

The von Neumann stability condition produces a necessary but not sufficient condition for stability (CUMINATO; MENEGUETTE, 1999).

Consider Δx and Δt the partitions in space and time, respectively, and $I = \sqrt{-1}$ the imaginary complex number. Let E_i, for $i = 1, ...N$, be the error at each mesh point in time step $t = 0$. Then we write E_i through a complex Fourier series (FORTUNA, 2012)

$$E_i = \sum_{n=1}^{N} a_n^0 \; e^{I\alpha_n (i\Delta x)}, \qquad \text{i = 1, ... N,} \tag{43}$$

where $\alpha_n = \dfrac{n\pi}{L}$ and $N\Delta x = L$.

The time dependence of the error E_i is incorporated through the amplitude $a_n^0 \to a_n^k$. It is assumed that the error tends to grow or decay exponentially with time, so the error, equation (43), in time k is written as

$$E_i^k = \sum_{n=0}^{N} e^{\gamma_n k} e^{I\alpha_n i\Delta x}. \tag{44}$$

Now E_i^k is the error at the position i and at the time step k.

The error, equation (44), is a propagation of harmonic waves of the type $e^{\gamma k} e^{I\xi i}$. In order for this propagation to be stable, the absolute value of the error amplitude must be less than or equal to unity (CUMINATO; MENEGUETTE, 1999; FORTUNA, 2012), i.e.,

$$|e^{\gamma k}| \leq 1. \tag{45}$$

Next, the von Neumann stability conditions will be obtained for the equations (11) and (12) when:

I) $F_1, F_2 \neq 0$ and $\tau_1, \tau_2 = 0$ (Predator-Prey system with reactive terms);

II) $F_1, F_2 = 0$, $\tau_1, \tau_2 \neq 0$ (Telegraph equations);

III) $F_1, F_2 \neq 0$ and $\tau_1, \tau_2 \neq 0$ (Telegraph Predator-Prey system). In this case the stability analysis will be obtained through numerical experiments.

Von Neumann conditions for a Predator-Prey system

Consider the following Diffusive Predator-Prey system

$$\frac{\partial S_1}{\partial t} = D_1 \frac{\partial^2 S_1}{\partial x^2} + a_1 S_1 - b_1 S_1^2 - c_1 S_1 S_2 \tag{46}$$

$$\frac{\partial S_2}{\partial t} = D_2 \frac{\partial^2 S_2}{\partial x^2} - a_2 S_2 + c_2 S_1 S_2, \tag{47}$$

where S_1, S_2 are the densities of prey and predator populations, respectively. The parameters a_1, a_2, c_1, c_2, and b_1 are positive constants described in equations (15) and (16), while $D_1 > 0$ and $D_2 > 0$ are the prey and predator diffusion rates, respectively. Note that the equations (46) and (47) are the equations (11) and (12) when $\tau_1 = \tau_2 = 0$.

For the discretization of the equations (46) and (47), we use progressive finite differences in time first-order derivative and central finite differences in space second-order derivative. Then the discretized versions of the equations (46) and (47) have the form

$$\begin{aligned} S_1|_P^{k+1} = S_1|_P^k + \sigma_1 \left(S_1|_E^k - 2S_1|_P^k + S_1|_W^k \right) \\ + \Delta t S_1|_P^k \left(a_1 - b_1 S_1|_P^k - c_1 S_2|_P^k \right) \end{aligned} \tag{48}$$

$$\begin{aligned} S_2|_P^{k+1} = S_2|_P^k + \sigma_2 \left(S_2|_E^k - 2S_2|_P^k + S_2|_W^k \right) \\ + \Delta t S_2|_P^k \left(-a_2 + c_2 S_1|_P^k \right) \end{aligned} \tag{49}$$

where $\sigma_j = \dfrac{\Delta t \, D_j}{\Delta x^2}$ for $j = 1, 2$.

Note that the equations (48) and (49) are non-linear, due to the reactive terms F_1 and F_2. On the other hand, the von Neumann superposition procedure is valid only for linear equation systems. Then it is necessary to linearize the equations (48) and (49).

It is assumed, in the nonlinear terms of (48) and (49), that the variables S_1 and S_2 are locally positive constants m_1 and m_2, respectively. From this hypothesis, it follows that the linear version of the equations (48) and (49) is given by

$$\begin{aligned} S_1|_P^{k+1} = S_1|_P^k + \sigma_1 \left(S_1|_E^k - 2S_1|_P^k + S_1|_W^k \right) \\ + \Delta t S_1|_P^k \left(a_1 - b_1 m_1 - c_1 m_2 \right) \end{aligned} \tag{50}$$

$$\begin{aligned} S_2|_P^{k+1} = S_2|_P^k + \sigma_2 \left(S_2|_E^k - 2S_2|_P^k + S_2|_W^k \right) \\ + \Delta t S_2|_P^k \left(-a_2 + c_2 m_1 \right). \end{aligned} \tag{51}$$

Assuming that $S_1|_P^k = S_2|_P^k = e^{\gamma k} e^{I\xi P}$, in equations (50) and (51), we obtain for the point P, in the time k,

$$e^{\gamma} = 1 - 4\sigma_1 \sin^2\left(\frac{\xi}{2}\right) + \Delta t \left(a_1 - b_1 m_1 - c_1 m_2 \right) \tag{52}$$

$$e^{\gamma} = 1 - 4\sigma_2 \sin^2\left(\frac{\xi}{2}\right) + \Delta t \left(-a_2 + c_2 m_1 \right). \tag{53}$$

The stability condition requires that $|e^{\gamma}| \leq 1$, so

$$-1 \leq 1 - 4\sigma_1 \sin^2\left(\frac{\xi}{2}\right) + \Delta t \left(a_1 - b_1 m_1 - c_1 m_2 \right) \leq 1 \tag{54}$$

$$-1 \leq 1 - 4\sigma_2 \sin^2\left(\frac{\xi}{2}\right) + \Delta t \left(-a_2 + c_2 m_1 \right) \leq 1. \tag{55}$$

Finally, after some algebraic manipulations, we get

$$0 \leq \Delta t \leq \frac{\Delta x^2}{2D_1 \sin^2\left(\frac{\xi}{2}\right) - \frac{\Delta x^2}{2}\left(a_1 - b_1 m_1 - c_1 m_2\right)} \quad (56)$$

$$0 \leq \Delta t \leq \frac{\Delta x^2}{2D_2 \sin^2\left(\frac{\xi}{2}\right) - \frac{\Delta x^2}{2}\left(-a_2 + c_2 m_1\right)}, \quad (57)$$

which are the von Neumann conditions for the predator-prey discretized equations (48) and (48), respectively. Note that the conditions in equations (56) and (57) impose restrictions on the spatial refinements Δx and temporal refinements Δt for stability in the numerical experiments.

Von Neumann conditions for a Telegraph system

Consider the telegraph equation system

$$\tau_j \frac{\partial^2 S_j}{\partial t^2} + \frac{\partial S_j}{\partial t} = D_j \frac{\partial^2 S_j}{\partial x^2}, \quad (58)$$

where $\tau_j > 0$ and $D_j > 0$ are delay and diffusion constants, respectively, for $j = 1, 2$.

Using the discretization schemes given in equations (17)-(19) in equation (58), it follows that

$$S_j\big|_P^{k+1} = \left(2 - \frac{\Delta t}{\tau_j} - \frac{2D_j \Delta t^2}{\Delta x^2 \tau_j}\right) S_j\big|_P^k$$

$$+ \frac{D_j \Delta t^2}{\Delta x^2 \tau_j}\left(S_j\big|_E^k + S_j\big|_W^k\right) - \left(1 - \frac{\Delta t}{\tau_j}\right) S_j\big|_P^{k-1}. \quad (59)$$

From the von Neumann hypothesis $S_j\big|_P^k = e^{\gamma k} e^{I\xi P}$, we get that

$$e^{\gamma} = 2 - \frac{\Delta t}{\tau_j} - \frac{2D_j \Delta t^2}{\tau_j \Delta x^2}\left(1 - \cos\xi\right) - \left(1 - \frac{\Delta t}{\tau_j}\right) e^{-\gamma}. \quad (60)$$

Multiplying by e^{γ} and making use of trigonometric transformations, the equation (60) is rewritten as

$$e^{2\gamma} - 2\beta_j e^{\gamma} + \left(1 - \frac{\Delta t}{\tau_j}\right) = 0, \quad (61)$$

where $\beta_j = 1 - 2\sigma_j \frac{\Delta t}{\tau_j} \sin^2\left(\frac{\xi}{2}\right) - \frac{\Delta t}{2\tau_j}$ and $\sigma_j = \frac{D_j \Delta t}{\Delta x^2}$, for $j = 1, 2$. Solving the roots of equation (61)

$$g_{1,2} = e^{\gamma} = \beta_j \pm \sqrt{\beta_j^2 - 1 + \frac{\Delta t}{\tau_j}}. \quad (62)$$

To analyze the roots of equation (62), consider the Lemma I.

Lemma I: *Let $x \in (0,1]$ and $a(x)$ be a real function defined by $a(x) = \frac{x}{2}$. If for each $x \in (0,1]$ we take $y \leq 1 - a(x)$, then $0 \leq \sqrt{y^2 - 1 + x} + y \leq 1$.*

Proof: Let y be a real number such that $y \leq 1 - \frac{x}{2}$ for all $x \in (0,1]$. Thus, we have $y \in \left[\frac{1}{2}, 1\right)$. So,

$$\begin{aligned} 0 \leq \sqrt{y^2 - 1 + x} + y &\leq \sqrt{\left(1 - \frac{x}{2}\right)^2 - 1 + x} + 1 - \frac{x}{2} \\ &= \sqrt{\frac{x^2}{4}} + 1 - \frac{x}{2} = 1. \end{aligned}$$

Therefore, $0 \leq \sqrt{y^2 - 1 + x} + y \leq 1$. □

In the context of Lemma I, consider the following cases:

Case I) $\beta_j^2 - 1 + \frac{\Delta t}{\tau_j} < 0$

In this case $\sqrt{\beta_j^2 - 1 + \frac{\Delta t}{\tau_j}}$ generates conjugate complex roots, that is,

$$g_{1,2} = \beta_j \pm i\sqrt{1 - \frac{\Delta t}{\tau_j} - \beta_j^2}. \quad (63)$$

Taking the norm of equation (63)

$$||g||^2 = \beta_j^2 + 1 - \frac{\Delta t}{\tau_j} - \beta_j^2 = 1 - \frac{\Delta t}{\tau_j} < 1, \text{if } 0 \leq \frac{\Delta t}{\tau_j} \leq 1. \quad (64)$$

So, in this case, when $0 \leq \frac{\Delta t}{\tau_j} \leq 1$ and $\beta_j^2 - 1 + \frac{\Delta t}{\tau_j} < 0$, by Von Neumann's criterion there is numerical convergence for the (59) system.

Case II) $\beta_j^2 - 1 + \frac{\Delta t}{\tau_j} \geq 0$

In this case, for $0 \leq \frac{\Delta t}{\tau_j} \leq 1$, equation (62) can result in $g_j = e^{\gamma} = 2\beta_j$, when $\frac{\Delta t}{\tau_j} = 1$, therefore we must limit the possible values of β_j. From Lemma I, we impose that

$$\frac{1}{2} \leq \beta_j \leq 1 - \frac{\Delta t}{2\tau_j}, \quad (65)$$

which results in

$$\frac{1}{2} \leq 1 - 2\sigma_j \frac{\Delta t}{\tau_j} \sin^2\left(\frac{\xi}{2}\right) \leq 1. \quad (66)$$

Solving the inequality of equation (66), it follows that

$$0 \leq \sigma_j \leq \frac{1}{4}. \quad (67)$$

Then, by Lemma I, if $0 < \frac{\Delta t}{\tau_j} \leq 1$ and $\beta_j^2 - 1 + \frac{\Delta t}{\tau_j} \geq 0$, the von Neumann stability condition of the discretized equation (59) is given by

$$0 \leq \sigma_j \leq \frac{1}{4}, \quad (68)$$

where $\sigma_j = \frac{D_j \Delta t}{\Delta x^2}$ for $j = 1, 2$.

Stability diagram for a Telegraph Predator-Prey system

In the case of equations (11) and (12), or in its discretized form given by the equations (23) and (29), which describe a Telegraph Predator-Prey system with diffusive, reactive, and delayed effects, it was not possible to obtain an analytical form for the von Neumann stability condition. In this context, numerical experiments will be carried out to obtain the stability diagram for the numerical scheme used.

Setting the reactive parameters $a_1 = 1\ s^{-1}$, $a_2 = 0.75\ s^{-1}$, $b_1 = 0.5\ m/s$, $c_1 = 0.5\ m/s$, and $c_2 = 0.5\ m/s$ (NATTI *et al.*, 2019), phase diagrams of the variables D_j, diffusibility coefficient, and τ_j, delay time, were constructed, for $j = 1,2$.

The phase diagrams show the regions of stability and instability of the PDE system, equations (11) and (12), for different values of Δt and Δx. It is important to note that $D_1 = D_2$ and $\tau_1 = \tau_2$ in all simulations, that is, there was no different diffusion or delay between the populations S_1 and S_2. In the following numerical experiments, the following initial and boundary conditions were considered

$$S_1(x,0) = S_1^0 = S_2(x,0) = S_2^0 = \begin{cases} 15;\ 24 \leq x \leq 26 \\ 0;\ \text{otherwise} \end{cases} \tag{69}$$

$$S_1(0,t) = S_1(50,t) = S_2(0,t) = S_2(50,t) = 0, \tag{70}$$

where $x \in [0,50]$ and $t \in [0,100]$.

All the simulations contained in this work were carried out in an Ubuntu operating system, where the codes were all programmed in FORTRAN 90 language and the images generated via Gnuplot software.

First, some simulations were carried out with different partitions of the temporal domain. Fixed $\Delta x = 0.1$, Figures 3 and 4 show the graphs of the numerical stability/instability regions, as a function of the diffusion, D_j, and the delay time, τ_j, of prey and predator populations, for two different values of Δt, $\Delta t = 0.002$ in Figure 3 and $\Delta t = 0.001$ in Figure 4.

Note that when refining the temporal domain, to a fixed Δx, the numerical stability region grows. See the values of D_j in Figures 3 and 4.

Now we set $\Delta t = 0.0015255$. Figures 5 and 6 show the graphs of the numerical stability/instability regions, as a function of the diffusion, D_j, and the delay time, τ_j, of prey and predator populations, for two different values of Δx, $\Delta x = 0.1$ in Figure 5 and $\Delta x = 0.025$ in Figure 6.

Figure 3 – Region of stability/instability for the Telegraph Predator-Prey system for refinements $\Delta x = 0.1$ and $\Delta t = 0.002$.

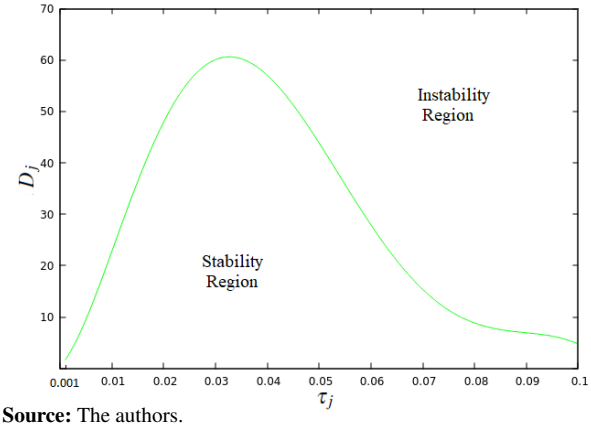

Source: The authors.

Figure 4 – Region of stability/instability for the Telegraph Predator-Prey system for refinements $\Delta x = 0.1$ and $\Delta t = 0.001$.

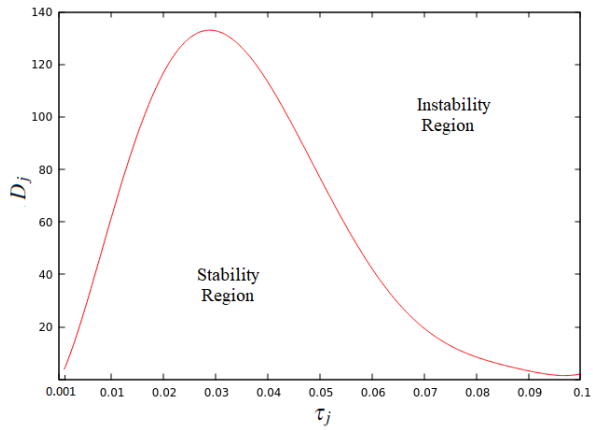

Source: The authors.

Figure 5 – Region of stability/instability for the Telegraph Predator-Prey system for refinements $\Delta x = 0.1$ and $\Delta t = 0.0015255$.

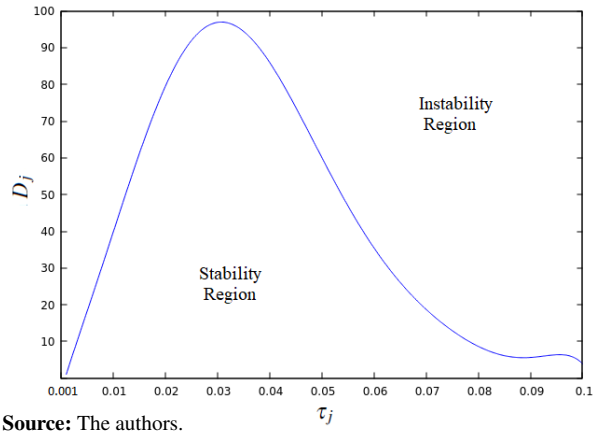

Source: The authors.

Note that when refining the spatial domain, to a fixed Δt, the numerical stability region decreases. See the values of D_j in Figures 5 and 6.

Figure 6 – Region of stability/instability for the Telegraph Predator-Prey system for refinements $\Delta x = 0.025$ and $\Delta t = 0.0015255$.

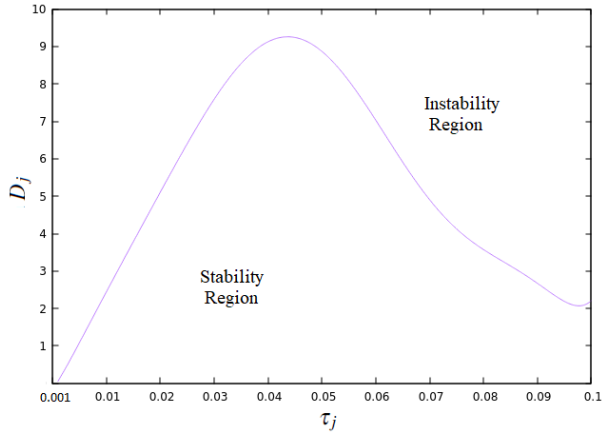

Source: The authors.

Numerical convergence analysis

The objective of this section is to analyze the convergence of the numerical scheme used to solve the model under study. In general, to verify numerical convergence, the Lax Equivalence Theorem must be satisfied (LAX; RICHTMYER, 1956; ROMEIRO *et al.*, 2021; STRIKWERDA, 2004).

Lax Equivalence Theorem: *For a consistent finite difference scheme of a well-posed initial value problem, stability is a necessary and sufficient condition for convergence.*

First, it is necessary to verify if the PDE system, equations (11) and (12), are well-posed, that is, if the problem in question has a solution and if it is unique. In the literature there are works on the existence and uniqueness of solutions of Telegraph equations (AYALA, 2012). There are also several works on the existence and uniqueness of Telegraph Predator-Prey systems, or more general Telegraph models (BOCIU; LASIECKA, 2010; CAVALCANTI; CAVALCANTI; FERREIRA, 2001; CAVALCANTI; CAVALCANTI; SORIANO, 2002; MUSTAFA, 2012; SHAOYONG, 1997).

There are also several works on numerical convergence of telegraph-type models (ATANGANA, 2015; EL-AZAB; EL-GAMEL, 2007). On the other hand, numerical convergence studies of Telegraph Predator-Prey models, with Reaction-diffusion-delay effects, are few and recent (CIRILO *et al.*, 2019). Then, a numerical study of mesh refinement is presented to evaluate the process of numerical convergence for this model.

Mesh refinement and convergence

Note that S_1 and S_2 are population densities of prey and predators, respectively, so to obtain the total population of prey and predators, in a time t, one must integrate S_1 and S_2 at the position coordinate x. This calculation is performed using the definite integral

$$P_j(t) = \int_{X_0}^{X_f} S_j(x,t)dx, \tag{71}$$

where P_1 and P_2 are the populations of prey and predator, respectively, at time t.

Let N_i be the number of partitions in the spatial domain, $x \in [X_0,\ X_f]$, and N_j the number of partitions in the temporal domain $t \in [T_0,\ T_f]$. Thus, we have the following relations

$$\Delta x = \frac{X_0 - X_f}{N_i - 1} \quad \text{and} \quad \Delta t = \frac{T_0 - T_f}{N_j - 1}. \tag{72}$$

Next, an analysis of the convergence of the numerical solution of the problem regarding the mesh refinement is performed. The Table 1 presents the values of the parameters used in the simulations. The initial and boundary conditions are those given earlier in equations (69) and (70).

Table 1 – Values used for model parameters in the numerical simulations

Parameters	Prey	Predator
$a_j\ (s^{-1})$	1.0	0.75
$b_j\ (m/s)$	0.5	0.0
$c_j\ (m/s)$	0.5	0.5
$D_j\ (m^2/s)$	1.0	1.0
$\tau_j\ (s)$	0.001	0.001
$T_0\ (s)$	0.0	0.0
$T_f\ (s)$	100.0	100.0
$X_0\ (m)$	0.0	0.0
$X_f\ (m)$	50.0	50.0

Source: The authors.

Table 2 presents numerical experiments for the solution of the discretized Telegraph Predator-Prey system (23)-(32), as a function of the mesh refinement. The process of population convergence is observed as a function of this refinement.

Numerical experiments on convergence in the Telegraph Predator-Prey system

In this subsection, two numerical experiments are carried out for the Telegraph Predator-Prey system (11)-(12) in order to better understand the stability/instability phase diagrams obtained in Figures 3-6.

Table 2 – Prey population $P_1(t)$ and predator population $P_2(t)$ of the Telegraph Predator-Prey model for various refinements Δx and Δt, at time $t = 100\,s$, with the parameters in Table 1.

$\Delta x(m)$	$\Delta t(s)$	$P_1(t=100)$	$P_2(t=100)$
5.0	0.002	62.69325	18.90470
3.5	0.002	65.13776	19.45726
2.0	0.002	70.27077	20.51610
1.0	0.002	71.68832	21.04255
0.75	0.00175	72.22790	21.17758
0.5	0.0015	72.56129	21.29889
0.1	0.001	73.13264	21.49681
0.05	0.0005	73.20856	21.52185
0.01	0.0001	73.26829	21.54183
0.005	0.00005	73.27579	21.54433
0.0025	0.000025	73.27954	21.54558

Source: The authors.

Let us consider the stability and instability regions obtained in Figure 5, when $\Delta t = 0.0015255$ and $\Delta x = 0.1$. Figure 7 presents these regions again. Figure 7 also shows two points, one in the region of stability of the numerical scheme and the other at the limit of the region of instability of the numerical scheme.

Figure 7 – Region of stability/instability for the Telegraph Predator-Prey system for refinements $\Delta x = 0.1$ and $\Delta t = 0.0015255$. The point $(0.05, 20)$ is in the stability region, while the point $(0.05, 61)$ is at the limit of the instability region.

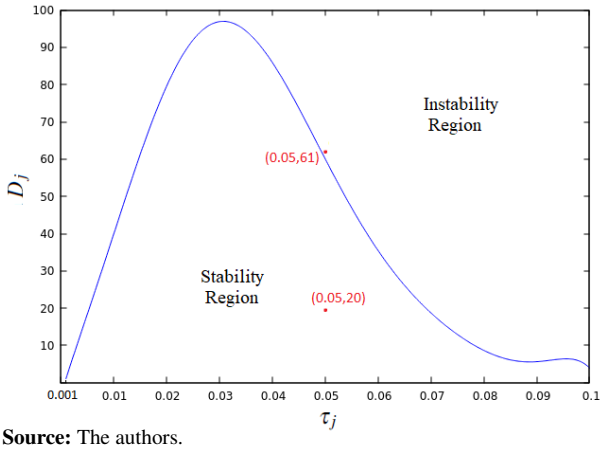

Source: The authors.

For the first numerical experimentation in this subsection, the values of the model parameters are presented in Table 3. Note that this simulation corresponds to the point in the stability region of Figure 7.

Figure 8 presents the population densities of prey and predators, in space coordinate, for the first numerical experiment at time $t = 100$.

Figure 9 presents the temporal variation, in $x = 25$, of the populations of prey and predators in the first numerical experiment.

Table 3 – Model parameter values for the first numerical experiment, corresponding to the point in the stability region of Figure 7

Parameters	Prey	Predator
$a_j\ (s^{-1})$	1.0	0.75
$b_j\ (m/s)$	0.5	0.0
$c_j\ (m/s)$	0.5	0.5
$D_j\ (m^2/s)$	20.0	20.0
$\tau_j\ (s)$	0.05	0.05

Source: The authors.

Figure 8 – Population densities of prey and predators of the Telegraph Predator-Prey model, in $t = 100$, corresponding to the first numerical experiment.

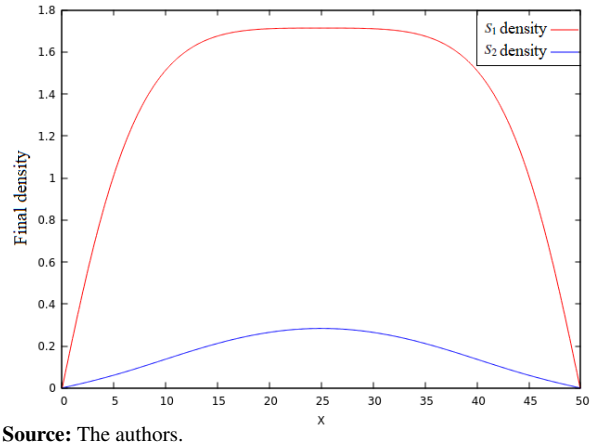

Source: The authors.

Figure 9 – Populations of prey and predators over time of the Telegraph Predator-Prey model, in $x = 25$, corresponding to the first numerical experiment.

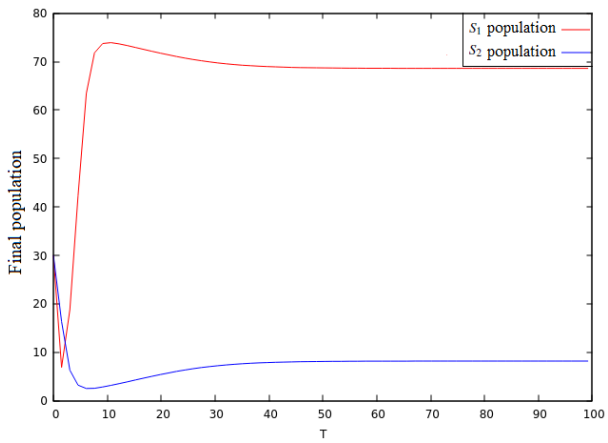

Source: The authors.

Figure 10 shows population densities of predator and prey in the entire spatial and temporal domain. Note that in this simulation there are no negative population densities.

Figure 10 – 3D graph of predator and prey population densities of the Telegraph Predator-Prey model corresponding to the first numerical experiment.

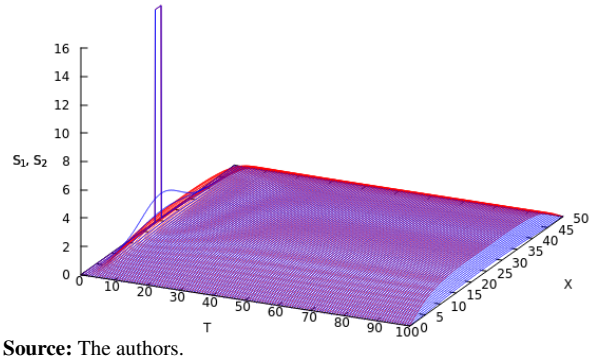

Source: The authors.

For the second numerical experiment in this subsection, the values of the model parameters are presented in Table 4. The second numerical experiment corresponds to the point at the limit of the instability region in Figure 7.

Table 4 – Model parameter values for the second numerical experiment, corresponding to the point at the limit of the instability region in Figure 7.

Parameters	Prey	Predator
$a_i\ (s^{-1})$	1.0	0.75
$b_i\ (m/s)$	0.5	0.0
$c_i\ (m/s)$	0.5	0.5
$D_i\ (m^2/s)$	61.0	61.0
$\tau_i\ (s)$	0.05	0.05

Source: The authors.

Figure 11 presents the population densities of prey and predators, in space coordinate, for the second numerical experiment at time $t = 100$. Note that the final population density of predators is zero, that is, the extinction of predators occurs.

Figure 12 presents the temporal variation, in $x = 25$, of prey and predators populations in the second numerical experiment.

The Figure 13 shows population densities of predator and prey in the entire spatial and temporal domain. It is observed that for some values of t there are negative population densities, as can be seen in Figure 14.

Note this behavior is unrealistic from a biological point of view. According to the numerical solution presented in the second experiment, given the initial condition (69), the prey population rapidly decreases, becomes negative and grows again until it reaches saturation. This is evidence of the instability of numerical solutions.

Figure 11 – Population densities of prey and predators of the Telegraph Predator-Prey model, in $t = 100$, corresponding to the second numerical experiment.

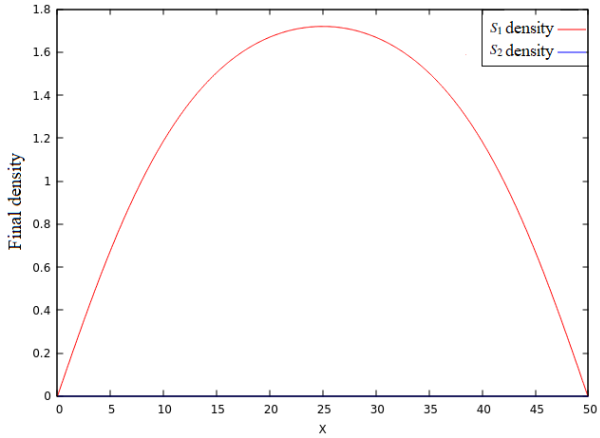

Source: The authors.

Figure 12 – Populations of prey and predators over time of the Telegraph Predator-Prey model, in $x = 25$, corresponding to the second numerical experiment.

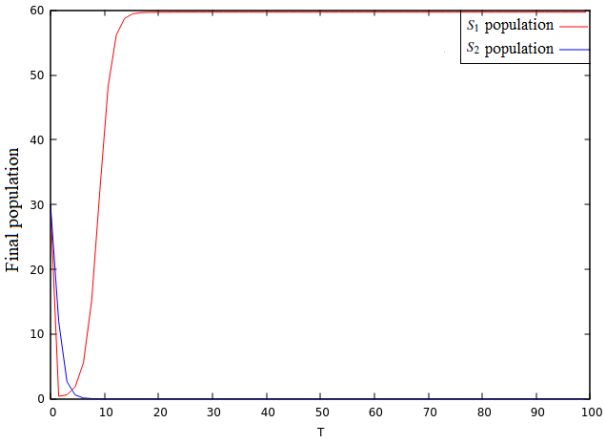

Source: The authors.

Figure 13 – 3D graph of predator and prey population densities of the Telegraph Predator-Prey model corresponding to the second numerical experiment.

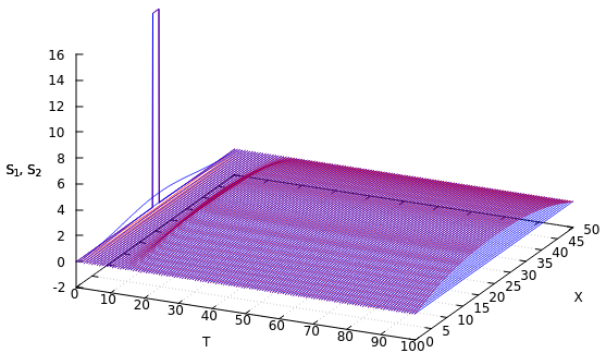

Source: The authors.

Figure 14 – Observation (first red line) of the spatial/temporal region where negative solutions for prey population density occur.

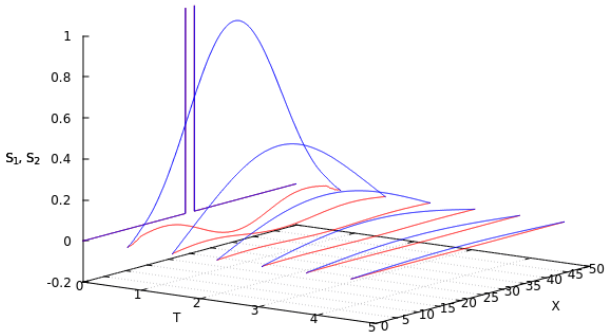

Source: The authors.

Conclusion

In this work, the mathematical modeling of the diffusive-reactive predator-prey system with delay (11)-(12) was performed. This model is also called Telegraph Predator-Prey system. Through numerical modeling, this EDP system was discretized by the Finite Difference method, equations (23)-(32).

First, it was verified that the discretized equations (23)-(32) were consistent with the PDEs (11)-(12) of the mathematical model.

In the sequence, through the von Neumann procedure, the numerical stability of systems simpler than the Telegraph Predator-Prey system was discussed. For the predator-prey system (46)-(47) and for the telegraph equation system (58) it was found that the numerical scheme used is conditionally stable, since the stability constraints (56)-(57) and (68) depend on the parameters of these models.

On the other hand, for the telegraph predator-prey system (11)-(12), it was not possible to obtain an analytical mathematical relationship for the von Neumann stability condition. Then, through numerical experiments, phase diagrams of the stability/instability regions were constructed as a function of the diffusion D_j and delay time τ_j parameters of the model (11)-(12), see Figures 3-6. Thus, it can be concluded that the telegraph predator-prey system (11)-(12) is also conditionally stable, depending on its diffusion, delay and reactive parameters.

Through numerical experiments again, the convergence of the numerical model was analyzed. Through the spatial and temporal refinement of the mesh, it was found that the prey and predator populations of the telegraph predator-prey system converged, as shown in Table 2.

Finally, it was possible to observe the numerical instabilities that occur in numerical simulations. In the phase diagram presented in Figure 7, two points were chosen, one in the region of stability of the numerical scheme and the other at the limit of the region of instability of the numerical scheme. It was found that when passing from the stability region to the instability region, negative fluctuations occur for population densities, which is an evidence of instability of numerical solutions, as can be seen in Figure 14.

Acknowledgments

The authors Kariston Stevan Luiz and Juniormar Organista was partly financed by the Coordination of Improvement of Higher Education Personnel (Capes), Brazil - Finance Code 001.

References

ABIDEMI, A.; ZAINIDDIN, Z. M.; AZIZ, N. A. B. Impact of control interventions on COVID-19 population dynamics in Malaysia: a mathematical study. *The European Physical Journal Plus*, Heidelberg, v. 136, n. 2, p. 1-35, 2021. DOI: https://doi.org/10.1140/epjp/s13360-021-01205-5.

ASH, T.; BENTO, A. M.; KAFFINE, D.; RAO, A.; BENTO, A. I. Disease-economy trade-offs under alternative epidemic control strategies. *Nature Communications*, London, v. 13, p. 3319, 2022. DOI: https://doi.org/10.1038/s41467-022-30642-8.

ATANGANA, A. On the stability and convergence of the time-fractional variable order telegraph equation. *Journal of Computational Physics*, San Diego, v. 293, p. 104-114, 2015.

AYALA, Y. S. S. Global existence and exponential stability for a coupled wave system. *Journal of Mathematical Sciences: Advances and Applications*, Allahabad, v. 16, p. 29-46, 2012.

BAZYKIN, A. D. Nonlinear dynamics of interacting populations. Amsterdam: World Scientific Publishing, 1998.

BEARUP, D.; PETROVSKAYA, N. B.; PETROVSKII, S. Some analytical and numerical approaches to understanding trap counts resulting from pest insect immigration. *Mathematical Biosciences*, London, v. 263, p. 143–160, 2015. DOI: https://doi.org/10.1016/j.mbs.2015.02.008.

BOCIU, L.; LASIECKA, I. Local Hadamard well-posedness for nonlinear wave equations with super-critical sources and damping. *Journal of Differential Equations*, Amsterdam, v. 249, p. 654-683, 2010. DOI: https://doi.org/10.1016/j.jde.2010.03.009.

BURDEN, R. L.; and FAIRES, J. D. *Análise numérica*. São Paulo: Cengage Learning, 2008.

CATTANEO, C.R. Sur une forme de l'équation de la chaleur éliminant le paradoxe de l'une propagation instantanée. *Comptes Rendus*, Grenoble, v. 247, n. 4, p. 431–433, 1958.

CAVALCANTI, M. M.; CAVALCANTI, V. N. D.; FERREIRA, J. Existence and uniform decay for nonlinear viscoelastic equation with strong damping. *Mathematical Methods in the Applied Sciences*, Stuttgart, v. 24, p. 1043-1053, 2001.

CAVALCANTI, M. M.; CAVALCANTI, V. N. D.; SORIANO, J. A. Exponential decay for the solution of semilinear viscoelastic wave equations with localized damping. *Electronic Journal of Differential Equations*, San Marcos, v. 44, p. 1-14, 2002.

CIRILO, E. R.; BARBA, A. N. D.; NATTI, P. L.; ROMEIRO, N. M. L. A numerical model based on the curvilinear coordinate system for the MAC method simplified. *Semina. Ciências Exatas e Tecnológicas*, Londrina, v. 39, n. 2, p. 87-98, 2018. DOI: https://doi.org/10.5433/1679-0375.2018v39n2p87.

CIRILO, E. R.; PETROVSKII, S. V.; ROMEIRO, N. M. L.; NATTI, P. L. Investigation into the critical domain problem for the reaction-telegraph equation using advanced numerical algorithms. *International Journal of Applied and Computational Mathematics*, New Delhi, v. 5, p. 1-15, 2019.

CIRILO, E. R.; NATTI, P. L.; ROMEIRO, N. M. L.; CANDEZANO, M. A. C.; POLO, J. M. P. One study of COVID-19 spreading at the United States - Brazil - Colombia. *Trends in Computational and Applied Mathematics*, São Carlos, v. 22, p. 435-452, 2021a.

CIRILO, E. R.; NATTI, P. L.; GODOI, P. H. V.; LERMA, A. A.; MATIAS, V. P.; ROMEIRO, N. M. L. COVID-19 in Londrina-PR: SEIR Model with Parameter Optimization. *SEMINA: Ciências Exatas e Tecnológicas*, Londrina, v. 42, n. 1Supl, p. 45-54, 2021b. DOI: https://doi.org/10.5433/1679-0375.2021v42n1Suplp45.

CRANK, J.; NICOLSON, P. A practical method for numerical evaluation of solutions of partial differential equations of the heat-conduction type. *Proceedings of the Cambridge Philosophical Society*, Cambridge, v. 43, p. 50-67, 1947.

CUMINATO, J. A.; MENEGUETTE, M. *Discretização de equações diferenciais parciais: técnicas de diferenças finitas.* Rio de Janeiro: SBMAC, 1999.

DE ROOS, A. M.; MC CAULEY, E.; WILSON, W. G. Mobility versus densirty-limited predador-prey dynamics on diferent spacial scales. *Proceedings of the Royal Society of London B: Biological Sciences*, London, v. 246, n. 1316, p. 117–122, 1991. DOI: https://doi.org/10.1098/rspb.1991.0132.

EL-AZAB, M.S.; EL-GAMEL, M. A numerical algorithm for the solution of telegraph equations. *Applied Mathematics and Computation*, New York, v. 190, p. 757-764, 2007. DOI: https://doi.org/10.1016/j.amc.2007.01.091.

FERREIRA, V. G.; CUMINATO, J. A.; TOMÉ, M. F.; FORTUNA, A. O.; MANGIAVACCHI, N.; CASTELO, A.; NONATO, L. G. Análise e implementação de modelos de turbulência K-ε para simulação de escoamentos imcompreessíveis envolvendo superfícies livres e rígidas. *Trends in Computational and Applied Mathematics*, São Carlos, v. 2, p. 81-90, 2001. DOI: https://doi.org/10.5540/tema.2001.02.01.0081.

FORTUNA, A. O. *Técnicas computacionais para dinâmica dos fluidos*. São Paulo: EDUSP, 2012.

GREENHALGH, D.; KHAN, Q. J. A.; PETTI, J. S. An eco-epidemiological predator–prey model where predators distinguish between susceptible and infected prey. *Mathematical Methods in the Applied Sciences*, London, v. 40, n. 1, p. 146–166, 2017. DOI: https://doi.org/10.1002/mma.3974.

GRIEBEL, M.; DORNSEIFER, T.; NEUNHOEFFER, T. *Numerical simulation in fluid dynamics: a practical introduction*. Philadelphia: Society for Industrial and Applied Mathematics, 1998.

HIRSCH, C. *Numerical computation of internal and external flows*. Oxford: John Wiley & Sons, 2007.

HOLLING, C. S. The components of predation as revealed by a study of small-mammal predation of the European pine sawfly. *The Canadian Entomologist*, Cambridge, v. 91, n. 5, p. 293–320, 1959a. DOI: https://doi.org/10.4039/ent91293-5.

HOLLING, C. S. Some characteristics of simple types of predation and parasitism. *The Canadian Entomologist*, Cambridge, v. 91, n. 7, p. 385–398, 1959b. DOI: https://doi.org/10.4039/Ent91385-7.

HUFFAKER, C. B. Experimental studies on predation: Dispersion factors and predator-prey oscillations. *Hilgardia*, Berkeley, v. 27, n. 14, p. 343–383, 1958. DOI: https://doi.org/10.3733/hilg.v27n14p343.

ISAACSON, E.; KELLER, H. B. *Analysis of numerical methods*. New York, Dover Publications, 1994.

KISHORE, N.; KAHN, R.; MARTINEZ, P. P.; DE SALAZAR, P. M.; MAHMUD, A. S.; BUCKEE, C. O. Lockdowns result in changes in human mobility which may impact the epidemiologic dynamics of SARS-CoV-2. *Scientific Reports*, London, v. 11, p. 6995, 2021. DOI: https://doi.org/10.1038/s41598-021-86297-w.

LAX, P. D.; RICHTMYER, R. D. Survey of the stability of linear finite difference equations. *Communications on Pure and Applied Mathematics*, New York, v. 9, p. 267-293, 1956. DOI: https://doi.org/10.1002/cpa.3160090206.

LEWIS, M.A.; PETROVSKII, S. V.; POTTS, J. R. *The mathematics behind biological invasions*, Switzerland: Springer International Publishing, 2016. (Interdisciplinary Applied Mathematics, v. 44).

LI, H.; LI, Y.; YANG, W. Existence and asymptotic behavior of positive solutions for a one-prey and two-competing-predators system with diffusion. *Nonlinear Analysis: Real World Applications*, Oxford, v. 27, p. 261–282, 2016. DOI: https://doi.org/10.1016/j.nonrwa.2015.07.010.

LI, S.; YUAN, S.; WANG, H. Disease transmission dynamics of an epidemiological predator-prey system in open advective environments. *Discrete and Continuous Dynamical Systems - B*, Springfield, v. 28, p. 1480-1502, 2023. DOI: https://doi.org/10.3934/dcdsb.2022131.

LOTKA, A. J. *Elements of physical biology*. Baltimore: World Scientific, 1925.

MENDEZ, V.; FEDOTOV, S.; HORSTHEMKE, W. *Reaction-transport systems: mesoscopic foundations, fronts and spatial instabilities*. Berlin: Springer-Verlag, 2010.

MICKENS, R. E.; JORDAN, P. M. A Positivity-preserving nonstandard finite difference scheme for the damped wave equation. *Numerical Methods for Partial Differential Equations*, Grenoble, v. 20, p. 639-649, 2003.

MUSTAFA, M. I. Well posedness and asymptotic behavior of a coupled system of nonlinear viscoelastic equations. *Nonlinear Analysis Real World Application*, London, v. 13, p. 452-463, 2012. DOI: https://doi.org/10.1016/j.nonrwa.2011.08.002.

NATTI, P. L.; ROMEIRO, N. M. L.; CIRILO, E. R.; NATTI, E. R. T.; OLIVEIRA, C. F.; SOBRINHO, A. S. O.; KITA, C. M. *Modelagem matemática e estabilidade de sistemas predador-presa*. In: GOMES, I. A. (org.). A produção do conhecimento nas ciências exatas e da terra 2. Ponta Grossa: Atena Editora, 2019. v. 2, p. 162-177. DOI: https://doi.org/10.22533/at.ed.39519040416.

OLIVEIRA, C. F; NATTI, P. L.; CIRILO, E. R.; ROMEIRO, N. M. L.; NATTI, E. R. T. Numerical stability of solitons waves through splices in quadratic optical media. *Acta Scientiarum. Technology*, Maringá, v. 42, p. e46881, 2019. DOI: https://doi.org/10.4025/actascitechnol.v42i1.46881.

PAUL, A.; LAURILA, T.; VUORINEN, V.; DIVINSKI, S. V. *Thermodynamics, diffusion and the kirkendall effect in solids. London: Springer, 2014.*

PAUL, A.; REJA, S.; KUNDU, S.; BHATTACHARYA, S. COVID-19 pandemic models revisited with a new proposal: Plenty of epidemiological models outcast the simple population dynamics solution. *Chaos, Solitons and Fractals*, Oxford, v. 144, p. 110697, 2021. DOI: https://doi.org/10.1016/j.chaos.2021.110697.

ROMEIRO, N. M. L.; BELINELLI, E. O.; Maganin, J.; NATTI, P.L.; CIRILO, E. R. Numerical study of different methods applied to the one-dimensional transient heat equation. *REMAT: Revista Eletrônica da Matemática*, Caxias do Sul, v. 7, p. e3012, 2021.DOI: https://doi.org/10.35819/remat2021v7i1id4767.

SAITA, T. M.; NATTI, P. L.; CIRILO, E. R.; ROMEIRO, N. M. L.; CANDEZANO, M. A. C.; ACUNA, R. A. B.; MORENO, L. C. G. Proposals for Sewage Management at Luruaco Lake, Colombia. *Environmental Engineering Science*, Larchmont, v. 38, n. 12, p. 1140-1148, 2021. DOI: https://doi.org/10.1089/ees.2020.0401.

SANGAY, J. C. A. *Aplicação do método de complementaridade mista para problemas parabólicos não lineares*. 2015. Dissertação (Mestrado) - Instituto de Ciências Exatas, Universidade Federal de Juiz de Fora, Juiz de Fora, 2015.

SHAOYONG, L. The asymptotic theory of semilinear perturbed telegraph equation and its application. *Applied Mathematics and Mechanics*, Shanghai, v. 18, p. 657-662, 1997. DOI: https://doi.org/10.1007/BF00127013.

STRIKWERDA, J. C. *Finite difference schemes and partial differential equations*. Philadelphia: SIAM, 2004.

TANSKY, M. Switching effect in prey-predator system. *Journal of Theoretical Biology*, Amsterdam, v. 70, n. 3, p. 263-271, 1978. DOI: https://doi.org/10.1016/0022-5193(78)90376-4.

TILLES, P. F. C.; PETROVSKII, S. V.; NATTI, P. L. A random walk description of individual animal movement accounting for periods of rest. *Royal Society Open Science*, London, v. 3, p. 160566, 2016. DOI: https://doi.org/10.1098/rsos.160566.

TILLES, P. F. C.; PETROVSKII, S. V.; NATTI, P. L. A random acceleration model of individual animal movement allowing for diffusive, superdiffusive and superballistic regimes. *Scientific Reports*, London, v. 7, p. 14364, 2017. DOI: https://doi.org/10.1038/s41598-017-14511-9.

VOLTERRA, V. Fluctuations in the abundance of a species considered mathematically. *Nature*, London, v. 118, p. 558–560, 1926. DOI: https://doi.org/10.1038/118558a0.

Received: June 16, 2022
Accepted: Nov. 11, 2022
Published: Nov. 29, 2022